An Analytical Solution to Nonlinear Flow Response of Soft Hair Beds

University of Texas at Austin Department of Physics
Undergraduate Thesis Zerrin Vural

Spring 2020

Supervising Professor: Dr. José Alvarado
Co-Supervising Professor: Dr. Philip Morrison

Abstract

Beds of passive, hair-like fibers can be found in many biological systems, including inside ourselves. Intestines, tongues, and blood vessels contain these types of surfaces, making us 'hairy' on the inside. A coupled elastoviscous problem arises when hairy surfaces are subjected to shear-driven Stokes flows. The hairs deform in response to fluid flows, and in turn, hair deformation affect fluid stresses. The theoretical model that accounts for the large-deformation flow response of a biomimetic model system of elastomer hair beds is known. However, the solution to the differo-integral equation of equilibrium governing the behavior of a bed of hairs immersed in fluid is difficult to uncover.

Here we develop a method to find the analytic solution to this equation of equilibrium. The time-independent equation of motion describing the bending of the hairs can be found by extending the pendulum problem for large angles to the case of bed hairs subject to Stokes flows. We consider the Hamiltonian formalism, analyze phase portraits, and utilize elliptic integrals to reduce the problem to a numerical problem. By these methods we find a solution that characterizes the hairs' shape by giving the angle with respect to the surface normal at any distance along the hair. Since it was found that biological hairy surfaces reduce fluid drag, angled hairs may be used in the design of integrated microfluidic components, such as diodes and pumps. Thus our solution would be useful to manufacture these devices.

1 Introduction

1.1 Physics Motivation

There are many intricate microscopic physical systems occurring inside our bodies that behave differently than larger models of that system. Fluid dynamics over such pileous surfaces behave differently on a microscopic scale compared to a macroscopic scale. While it is easy to imagine a stream flowing over a bed of underwater grasses, its less likely to consider the physics of fluid flow over microscopic hairy surfaces that line our own blood vessels, taste buds, or stomachs. However, small hairs ($\sim$ 1 to 100 μn) are found on brush-border microvilli, papillae of tongues, primary cilia of kidney cells, and hyaluronans of blood vessels' glycocalyx [1]. As fluid flows over these surfaces, the soft beds of hair elicit a nonlinear response of the fluid flow. Fluid flow around flexible structures is ubiquitous in nature. For example, leaves on a tree deform to reduce drag forces of wind [2]. This nonlinear deformation is called reconfiguration. Studies on reconfiguration have largely been done when inertial effects are greater than viscous effects, or at high Reynolds (Re) numbers [3]. Re is a dimensionless constant used in fluid dynamics that describes flow. It is the ratio of inertial forces to viscous forces. The physics of fluid flows over the small hairs is characterized by low Re, where viscous forces dominate. How reconfiguration is manifested at low Re remains poorly understood.

Dr. José Alvarado investigated the system of deformable hairs subject to low-Re fluid flow by mounting elastomer hair beds onto the inner rotor of a Taylor-Couette geometry [1]. From this experiment, a differential equation governing the bending of the hair submersed in fluid was derived, but the solution for this was not yet found. Besides gaining a better understanding of the motion of small hairs in fluids and reconfiguration effects at low Re the findings of this study could be seen in designs of diode, pumps and other microfluidic devices. This could be implemented in medical devices, among other applications of microfluidics.

1.2 Theoretical Background

The rheometry experiment allowed for the determination of shear stress τ as a nonlinear function of velocity v. Figure 1 a. depicts a stationary bed of hair immersed in fluid opposite to a smooth surface. In Figure 1 b. the opposite surface moves with velocity in the x-direction, and shows how fluid flow affects hair deformation in this model. No slip boundary conditions hold at the top surface, meaning that the fluid will have zero velocity relative to the moving top surface. Additionally no slip boundary conditions hold at $z = h$, or at the tips of the hairs. Elastoviscous coupling is observed as fluid flow causes the hairs to bend, thus position of the hair-tip plane h depends on shear stress τ. Shear forces are defined as being parallel to the surface. The model assumes zero flow (zero fluid stress) around the hair except at the tip.

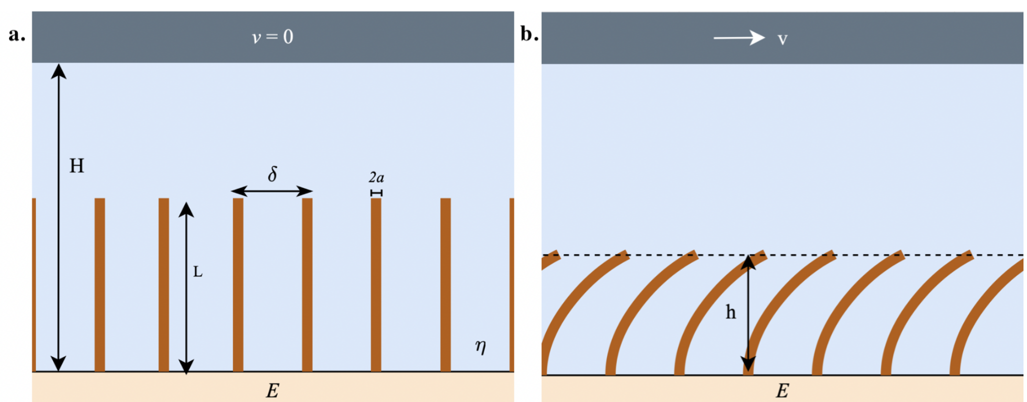

Figure 1: **a.** Schematic of the physical model of elastic hair bed when there is no fluid flow. The physical quantities depicted are: channel height H, hair length L, hair separation δ, hair elastic modulus E, hair diameter $2a$, and fluid viscosity η. **b.** Schematic of the physical model with plate velocity v, depicting reconfiguration. Hair height is now h, and fluid flows is between the gap of width $H - h$.

The elastoviscous coupling can be characterized by the Area-specific impedance Z. This is the ratio of shear stress to velocity, and can be thought of as how difficult it is to displace an object. For example, moving an sphere of radius r though a viscous medium requires a force $F_{drag} = 6\pi\eta r v$, where η is viscosity. To define a function $Z(v)$ for the system of the hairs, it was assumed the hairs deform identically, and therefore we can consider the model of a single hair as shown in Figure 2. Position along the hair is defined as the curvilinear coordinate s ranging from $s = 0$ at the base to $s = L$ at the tip. The angle that any point s along the hair differs from vertical is $\theta(s)$. This characterizes the shape of the hair. The hair-tip plane is given by $h(\theta(s)) = \int_0^L \cos(\theta(s))ds$. In the system of the hairs, h contributes to changes in the impedance. Z is defined as

$$Z(v) = \frac{\tau(v)}{v} = \frac{\eta}{H - h(v)} \tag{1}$$

The diameter of the hair is $2a$ and δ measures the hair separation thus the hair packing fraction is given by $\phi \cong a^2/\delta^2$. Force is given by the product of fluid shear stress, given by Equation (1), and fiber area, $\pi\delta^2 = \pi a^2/\phi$.

$$F = \frac{\pi a^2}{\phi}\tau = \frac{\pi a^2}{\phi}\frac{\eta v}{H - \int_0^L \cos\theta(s)} \tag{2}$$

The second order differential equation of the deflection curve of hair when subjected to lateral forces is called the bending moment [4] $M = EI\frac{d^2\theta}{ds^2}$, measured in the z-direction, where the second area moment of the hair's cross section is $I = (\pi/4)a^4$, and E is the elastic modulus. Force balance along the z-direction gives rise to the nonlinear differo-integral equation:

$$0 = EI\frac{d^2\theta(s)}{ds^2} + \frac{\pi a^2}{\phi}\frac{\eta v \cos\theta(s)}{H - \int_0^L \cos\theta(s)} \tag{3}$$

We have a boundary value problem for $\theta(s)$, the angle of bending at a certain position along the hair, s. This system is defined at an initial time

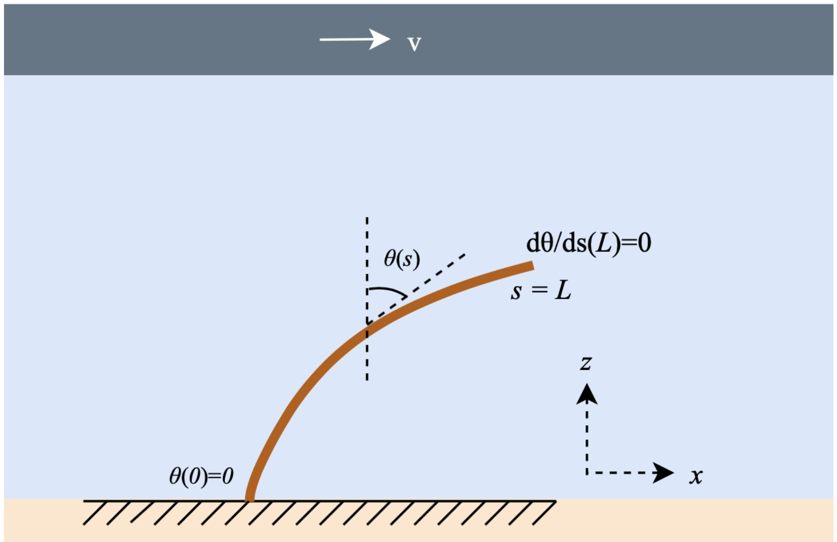

Figure 2: Schematic depicting reconfiguration of one hair. Hair shape can be described by $\theta(s)$, the angle that a tangent line at curvilinear distance s along the hair differs from vertical. Boundary conditions are shown. We have that the hair is anchored to the base such that $\theta(0) = 0$, and at the tip ($s = L$) the angle the hair differs from the vertical is not changing.

when the hair of length L has already been subjected to fluid flow and is thus in its reconfigured form. The base of the hair is anchored perpendicularly, therefore $\theta(0) = 0$. At the end of the hair the angle is not changing $\frac{d\theta}{ds}|_{s=L} = 0$.

The initial value problem is somewhat undefined in that only the initial angle at $s = 0$ is known, while the differential of the angle is currently unknown, $\frac{d\theta}{ds}|_{s=0} =: \theta_0'$. We will be able to obtain this value in the solution.

$$\text{Initial Conditions:} \qquad \theta(0) = 0 \quad \text{and} \quad \frac{d\theta}{ds}|_{s=0} =: \theta_0'$$

$$\text{Boundary Conditions:} \quad \theta(0) = 0 \quad \text{and} \quad \frac{d\theta}{ds}|_{s=L} = 0$$

In the following sections we will go through the steps in order to analytically solve equation (3) with the goal of finding an expression for $\theta(s)$ to be able to define the bending of small hairs in low-Re fluid flow. This happens to be an inverted pendulum problem, and therefore we find it conductive to compare the system of the hair to the classical pendulum problem beyond small angle approximations.

2 Background Concepts and the Large Angle Pendulum

In this section we will outline the pendulum problem beyond the small angle approximation, and explain useful concepts needed to solve the problem of hair beds subject to shear-driven forces.

2.1 Hamiltonian Systems

In classical mechanics conserved quantities are valuable in their use of characterizing a system. A Hamiltonian system with one degree of freedom is described by its Hamiltonian function $H(x(t), p(t))$ where x is generalized position coordinates and p represents generalized momentum,

$$\dot{x}_i = \frac{\partial H}{\partial p_i}$$

$$\dot{p}_i = \frac{\partial H}{\partial x_i}$$

where $i = 1, 2, ...n$ is the number of degrees of freedom [5]. The Hamiltonian is the total energy: the sum of the kinetic K and potential V energy of the system. This quantity is a constant of the motion and is conserved. In a planar system we have

$$H(x, p) = \frac{1}{2}\frac{p^2}{m} + V(x) \tag{4}$$

Here $\frac{1}{2}p^2$ is the kinetic energy and $V(x)$ is the potential energy. Considering a state space of (x, p), the differential equations of this system are

$$\begin{aligned} \dot{x} =& \frac{\partial H}{\partial p} = \frac{p}{m} \\ \dot{p} =& \frac{\partial H}{\partial p} = \frac{dV}{dx} \end{aligned}$$

Since $F = -dV/dx$, we get Newton's Second Law from $F = \dot{p} = m\ddot{x}$ from substituting the equations above.

2.2 Elliptic Integrals

Elliptic integrals are integrals of the form

$$f(x) = \int \frac{A(x) + B(x)}{C(x) + D(x)\sqrt{S(x)}}$$

where S(x) is a polynomial of degree 3 or 4 in x, and A(x), B(x), C(x), D(x) are polynomials of x [6]. Elliptic integrals are found in electrostatics, mechanics, number theory, and ODEs and PDEs, among other applications. Specifically, they are useful in finding the position of a pendulum beyond the small angle approximation. Elliptic integrals are unique in that they cannot be expressed in terms of elementary functions. However, they can be reduced into one of three Legendre forms of elliptic integrals which form a canonical set: elliptic integral of the first, second, and third kinds. These integrals are so named after ellipses because the elliptic integral of the second kind is used to evaluate the arc length of an ellipse.

The incomplete elliptic integral of the first kind is defined as

$$F(\phi|k^2) = \int_0^\phi \frac{1}{\sqrt{1 - k^2 \sin^2 \phi}} d\theta \tag{5}$$

where the modulus, k, goes between $0 < k^2 < 1$, and ϕ is defined as the amplitude. When ϕ is set to be $\pi/2$, or $\sin\phi = 1$, the elliptic integral is said to be complete since this is the maximum that the upper limit of integration can be. There are many methods for finding solutions to the incomplete elliptic integral of the first kind. Among them are use of Legendre polynomials, numerical methods, and series expansion. They can be found in integral tables.

2.3 The Classical Pendulum

Now we will consider the case of the pendulum. This system is made up of a mass m suspended from a string of negligible weight and length l. The mass can be displaced from equilibrium by being initially lifted to one side and then let go of so that it is able to swing back and fourth in a vertical plane under the gravitational influence. The gravitational influence is known as the restoring force, causing the pendulum to oscillate around its equilibrium position.

By making the assumptions that there is no energy loss due to air resistance or friction about the pivot, the point mass will oscillate at a constant amplitude equal to the initial displacement. This system is often referred to as a simple gravitational pendulum and is illustrated in Figure 3. Let θ be the angle between the pendulum and the downward vertical. The potential energy is zero at the pendulum's lowest point, $\theta = 0$, the equilibrium position. The position of the pendulum is described by $\theta(t)$, the angle of displacement from vertical as a function of time. The initial conditions where the pendulum is released at an initial angle are as follows:

$$\theta(0) = \theta_0 \quad \text{and} \quad \tfrac{d\theta}{dt}|_{t=0} = 0$$

Through Hamiltonian analysis we can arrive at the equation of motion for the pendulum. Since there is no loss of friction, the total energy is the sum of potential and kinetic energy and energy is conserved. The pendulum

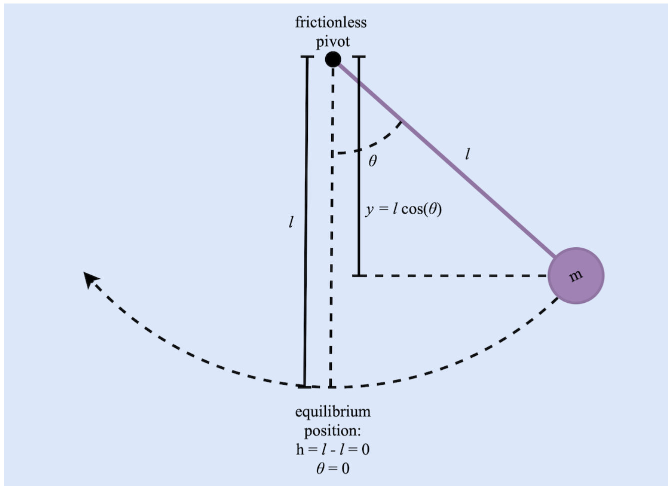

Figure 3: Diagram of a simple gravitational pendulum mounted by a frictionless pivot, allowing the mass m to swing from side to side with the same amplitude. The relevant physical quantities depicted are the lengh of the string l, the angle the string makes with vertical θ, the vertical distance from the pivot y. The vertical distance from the mass' equilibrium position h will be the variable used to measure the system's potential energy, and can be found by $h = l - y\cos\theta$.

problem and the hair problem are both 1 dimensional systems with forces that depend only on position. This means that the potential energy has a value at every point, and is related to the force by $F = -dV/dx$. We can write the Hamiltonian for the pendulum from Equation (4) since $p = mv$ and potential energy is mgh where g is the acceleration due to gravity and h is the vertical displacement from the equilibrium position at $\theta = 0$. Note that $H = E_{total}$.

$$H = K + V = \frac{1}{2}mv^2 + mgh \tag{6}$$

Using the formula for arc length, $s = l\theta$, we can rewrite the equation for kinetic energy in terms of angular velocity $v = \frac{ds}{dt} = l\frac{d\theta}{dt}$. So here

$$K = \frac{ml^2}{2}\left(\frac{d\theta}{dt}\right)^2$$

An expression for the h can be obtained in terms of y, the vertical distance of the mass from the pivot. When the pendulum is swinging through some angle, then $y = l\cos\theta$. The change in height h is the difference between l, the length of the string, and y. Thus $h = l(1-\cos\theta)$ Potential energy therefore becomes

$$V = mgl(1 - cos\theta)$$

The Hamiltonian function can be set to some constant value of energy due to conservation. Setting H to the initial energy E_0 allows us to use initial conditions to derive the pendulum's equation of motion. Evaluating E_0 at $t = 0$ and using conservation gives

$$E_0 = mgl(1-\cos\theta_0) = \frac{ml^2}{2}\left(\frac{d\theta}{dt}\right)^2 + mgl(1-\cos\theta) \tag{7}$$

Solving for $d\theta/dt$ gives

$$\frac{d\theta}{dt} = \sqrt{\frac{2g}{l}(\cos\theta - \cos\theta_0)} \tag{8}$$

We can differentiate both sides with respect to t. With chain rule we have

$$\frac{d^2\theta}{dt^2} = \frac{-\frac{g}{l}\sin\theta}{\sqrt{\frac{2g}{l}(\cos\theta - \cos\theta_0)}}\frac{d\theta}{dt}$$

$$\frac{d^2\theta}{dt^2} = \frac{-\frac{g}{l}\sin(\theta)}{\sqrt{\frac{2g}{l}(\cos\theta - \cos\theta_0)}}\sqrt{\frac{2g}{l}(\cos\theta - \cos\theta_0)}$$

$$\frac{d^2\theta}{dt^2} = -\frac{g}{l}\sin\theta$$

The differential equation of motion for the pendulum is then:

$$0 = \frac{d^2\theta}{dt^2} + \frac{g}{l}\sin(\theta) \tag{9}$$

For small angle oscillations the approximation $\sin\theta \approx \theta$ can be used which yields a linear differential equation for a harmonic oscillator. For this case the solution is easily found to be $\theta(t) = \theta_0 \cos\left(\sqrt{\frac{g}{l}}t\right)$. To find solutions of the pendulum's differential equation of motion beyond the small angle approximation requires more insight.

2.4 Solution for the Large Angle Pendulum

To find solutions of Equation (9) beyond the small angle approximation requires more insight [7]. The period T can be computed for this case by consider an inversion of the angular velocity (Equation (8)) and can help us to determine the equation of motion beyond the small angle approximation.

$$\frac{dt}{d\theta} = \sqrt{\frac{l}{2g}\frac{1}{(\cos\theta - \cos\theta_0)}} \tag{10}$$

We can integrate this over the time it takes to complete a full cycle of motion: $T = t(\theta_0 \to 0 \to -\theta_0 \to 0 \to \theta_0)$, or we can simplify this to four times the quarter cycle $T = 4t(\theta_0 \to 0)$.

$$\int_0^T dt = 4\sqrt{\frac{2g}{l}}\int_0^{\theta_0} \frac{1}{\sqrt{\cos\theta - \cos\theta_0}} d\theta \tag{11}$$

This is an improper integral since the integrand becomes undefined when $\theta = \theta_0$. To avoid this, we can use the double angle formula $\cos\theta = 1 - 2\sin^2(\theta/2)$.

$$\int_0^T dt = 4\sqrt{\frac{2g}{l}}\int_0^{\theta_0} \frac{1}{\sqrt{\sin^2(\theta_0/2) - \sin^2(\theta/2)}} d\theta \tag{12}$$

It is useful to rewrite this integral in terms of $\sin\phi = \frac{\sin(\theta/2)}{\sin(\theta_0/2)}$ and integrate with respect to ϕ. In one full oscillation on the pendulum, ϕ goes from 0 to 2π, thus a fourth of that allows for us to integrate from 0 to $\pi/2$. This change of variables allows for the right hand side to be in the form of a complete elliptic integral of the first kind as defined in Equation (5) where $k = \sin(\theta_0/2)$.

$$T = 4\sqrt{\frac{2g}{l}} \int_0^{\pi/2} \frac{1}{\sqrt{1 - k^2 \sin^2(\phi)}} d\phi \tag{13}$$

This is form is not improper because $k < 1$ for $|\theta_0| < \pi$, and therefore also for $|\phi| < \pi/2$. Now as an elliptic integral, it is possible to evaluate by series expansion or numerically. Furthermore, solutions can be found in integral tables [8].

This would give us the equation $T(\theta)$, the period of oscillation of the pendulum in terms of the angle it subtends. Then we can perform an Abel Transformation, making use of a given a known function of the energy, $T(E_0, \theta)$, to invert the equation to find the solution that describes the motion of the pendulum $\theta(t)$.

2.5 Phase Portraits

A phase portrait is a plot of trajectories in the (x, p)-plane which are parametric curves of the solutions to a differential equation. This plot is a visualization of how the vector field of a dynamic system looks at some point in time. Phase portraits can be used to graphically represent and predict how solutions of a system will behave in the long term. Critical points will be located along the $p = 0$-axis, where x-values along this axis correspond to saddle points or center points depending on whether the potential is at a local minimum or maximum respectively. A level set, $H(x, p)$ corresponds to a line or closed curve in the phase plane along which $V(x) = H(x, p)$ at any x value. They are often referred to as energy curves since the energy stays constant along these lines. Phase portraits are especially useful because for any conservative system, we can plot trajectories without having to find explicit solutions to the differential equation of motion.

2.6 Phase Portrait for The Pendulum

For the pendulum, we can plot $d\theta/dt$ versus $\theta(t)$ to see the trajectories that result from Equation (9). Assuming $g/l = 1$ for simplicity, we have that

$$\ddot{\theta} = -\sin(\theta) \tag{14}$$

Rewriting $d\theta/dt$ as velocity $v(t)$, it follows that

$$\begin{aligned}\dot{\theta}(t) =& v(t) = -\cos\theta \\ \dot{v}(t) =& -\sin(\theta)\end{aligned}$$

The rate of change at any point in time can be found for both variables. Now we can plot angular velocity versus angular displacement as a vector field as shown in Figure 4 b. Then we can follow the trajectory of a pendulum being released at some initial angle. Closed trajectories in the phase plane, such as the yellow path in Figure 4 b., corresponds to a system with periodic motion. This is the pendulum oscillating with amplitudes less than π. The closed trajectories centered at $(-2\pi, 0)$ and $(2\pi, 0)$ represent the same motion, since a shift of 2π results in the same angle.

If the pendulum has a strong enough velocity, it results in the pendulum swinging completely around the pivot, rather than oscillating back and fourth. This motion is represented by the wavy lines at the top and bottom of the graph representing clockwise and counterclockwise rotation respectively. The red trajectory in Figure 4 highlights continuous clockwise rotation about the pivot. When the pendulum has enough energy to swing all the way to vertical, but not enough to continue swinging in the same direction, it changes direction and swings to vertical once again. This motion corresponds to the orange lines in the phase portrait. This trajectory is called the separatrix because it separates the phase space into two regions in which the behavior of the solutions are different as $t \to \pm\infty$: those inside the separatrix describe oscillating motion, and those outside it describe the pendulum continuously

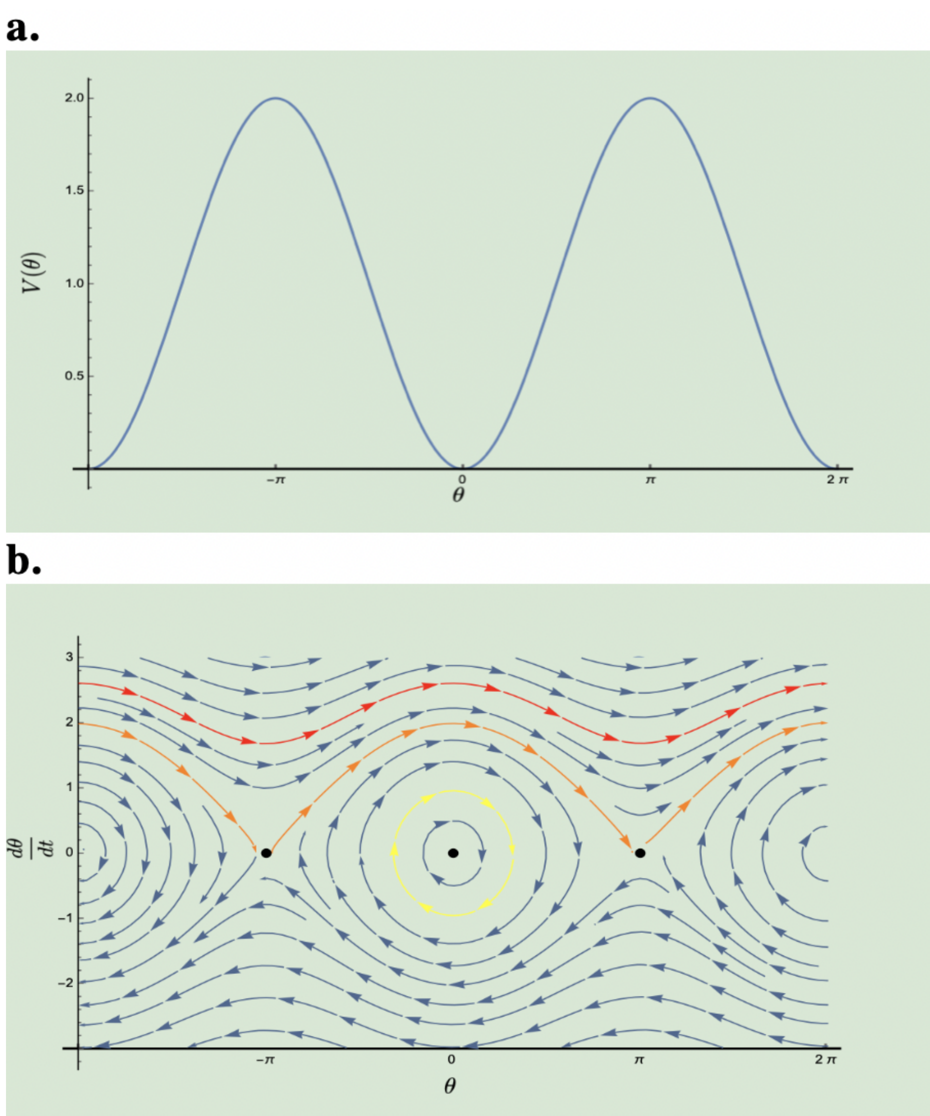

Figure 4: **a.** Potential energy for the pendulum graphed as $1 - \cos\theta$ for simplicity. **b.** Vector field plotting $d\theta/dt$ versus θ for a pendulum outlining the phase trajectories for different energy values. The red path corresponds to a pendulum swinging completely around the pivot in a clockwise direction. The orange path highlights the separatrix. The yellow path corresponds to oscillating motion. $v(\theta) = \sin(\theta)$.

swinging in the one direction [9]. Figure 5 isolates different possible paths of motion for a pendulum and the phase trajectory that corresponds to each case is shown above it.

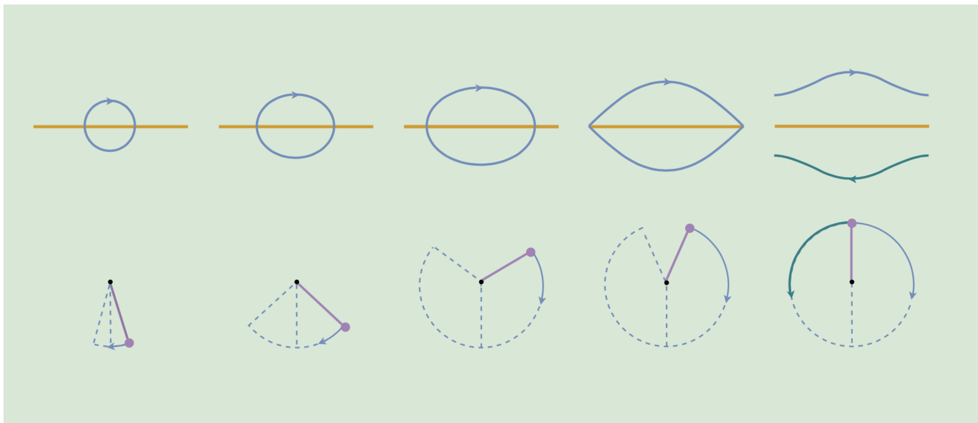

Figure 5: Phase trajectories corresponding to different arcs of a pendulum. If the amplitude of a the pendulum is less than π, the phase trajectory is a closed curve. As the amplitude increases, the period of the pendulum increases.

2.7 Connection to Hamiltonian

From the Hamiltonian function we can see that each curve represents an energy level surface [10]. Now let E be any energy of the Hamiltonian. From Equation (4) and letting our position coordinate x be θ in the context of the pendulum, we have

$$E = \frac{m}{2}\dot{\theta}^2 + V(\theta) \tag{15}$$

This gives a relation between $\dot{\theta}$ and θ corresponding to each value of total energy E. Solving for $\dot{\theta}$ gives

$$\dot{\theta} = \frac{d\theta}{dt} = \pm\sqrt{\frac{2}{m}(E - V(\theta))} \tag{16}$$

Thus, we can plot phase portraits, $\dot{\theta}$ vs θ, corresponding to certain E values.

This gives us another way to solve the pendulum equation by giving an equivalent form of Equation (8). An $n = 1$ degree of freedom Hamiltonian system has the property that it is completely intergrable. Therefore we apply separation of variables to get

$$\int_0^t dt = \int_{\theta(0)}^{\theta(t)} \frac{dx}{\sqrt{\frac{2}{m}(E - V(\theta))}} \tag{17}$$

It is helpful to continue to think of the oscillating pendulum, for which a given value of energy corresponds to a circular curve in the region around a stable equilibrium point and enclosed by separatrices. At $\dot{\theta} = p = 0$ we know the pendulum changes direction. This occurs at two points, θ_1 and θ_2. At this point, it is also implied that $E = V(\theta_1) = V(\theta_2)$. For the pendulum, $V(\theta) = mgl(1 - \cos\theta)$. Let $\bar{E} = E - 1$ Therefore to solve for position we need to solve specifically:

$$T(E, \theta) = 2\int_{\theta_1}^{\theta_2} \frac{dx}{\sqrt{\frac{2}{m}(\bar{E} + mgl\cos\theta)}} \tag{18}$$

The right hand side can be expressed as an incomplete elliptic integral of the first kind, giving the same result as Equation (13).

3 Solving Nonlinear Flow Response of Soft Hair Beds

Now we will apply the pendulum analogy to our system of the tiny hairs. Here we outline an analytical method to reduce Equation (3) to a numerical problem with the goal of finding $\theta(s)$ which will describe the bending of the hair along its arc length.

3.1 Pendulum to Hair Bed Analogy

Recall Equation (3)

$$0 = EI\frac{d^2\theta(s)}{ds^2} + \frac{\pi a^2}{\phi}\frac{\eta v\cos\theta(s)}{H - \int_0^L \cos\theta(s)} \tag{19}$$

This equation can be put into a form similar to the differential equation for the pendulum (Equation (9)). To simplify into this form initially, we will fix $h(\theta(s)) = \int_0^L \cos\theta(s)ds$ to be at s' so then $h(\theta(s')) = \int_0^L \cos\theta(s')ds'$. Letting $\hat{s} = s/L$, and $\hat{\theta}(\hat{s}) = \theta(s)$ gives

$$0 = EI\frac{d^2\hat{\theta}}{d\hat{s}^2} + \frac{\pi a^2}{\phi}\frac{L^2\eta v\cos\hat{\theta}}{H - L\int_0^1 \cos\hat{\theta}(\hat{s}')ds'} \tag{20}$$

We can isolate the second derivative term and gather the constants into one term

$$\frac{d^2\hat{\theta}}{d\hat{s}^2} + \frac{\pi a^2 L^2\eta v}{EIH\phi}\frac{\cos\hat{\theta}}{1 - \frac{L}{H}\int_0^1 \cos\hat{\theta}(\hat{s}')ds'} \tag{21}$$

Define the constant term to be

$$\omega^2 = \frac{\pi a^2 L^2\eta v}{EIH\phi} \tag{22}$$

Letting $\epsilon = \frac{H}{L}$ and defining

$$\omega_\epsilon^2 = \frac{\omega^2}{1 - \epsilon \int_0^1 \cos \hat{\theta}(\hat{s}') ds'} \tag{23}$$

or

$$\frac{\omega^2}{\omega_\epsilon^2} = 1 - \epsilon \int_0^1 \cos\left(\hat{\theta}(\hat{s}')\right) ds' \tag{24}$$

We will drop the 'hats' moving forward to avoid clutter. Now we have an equation similar to Equation (9) with $\cos\theta$ in place of $\sin\theta$.

$$0 = \frac{d^2\theta}{dt^2} + \omega_\epsilon^2 \cos\theta \tag{25}$$

Recall the differential equation has the following conditions, now with $L = 1$ from the change of variables

Initial Conditions: $\theta(0) = 0$ and $\frac{d\theta}{ds}|_{s=0} =: \theta_0'$

Boundary Conditions: $\theta(0) = 0$ and $\frac{d\theta}{ds}|_{s=1} = 0$

The Hamiltonian of this system, which we will call $\mathcal{E}$ takes the form of Equation (4). Figure 6 depicts how energy values for the hair resemble the case of the oscillating pendulum. Since $F = \ddot{\theta} = -dV/d\theta$ the potential can be found using Equation (25): $V(\theta) = \omega_\epsilon^2 \sin\theta$

$$\mathcal{E} = \frac{1}{2}\left(\frac{d\theta}{ds}\right)^2 + \omega_\epsilon^2 \sin\theta \tag{26}$$

The conservation of the energy can be proved by showing that the derivative of the Hamiltonian is zero since Equation (25) equals zero.

$$\frac{d\mathcal{E}}{ds} = \frac{d^2\theta}{ds^2}\frac{d\theta}{ds} + \omega_\epsilon^2 \cos\theta \frac{d\theta}{ds} = \frac{d\theta}{ds}\left(\frac{d^2\theta}{dt^2} + \omega_\epsilon^2 \cos\theta\right) = 0 \tag{27}$$

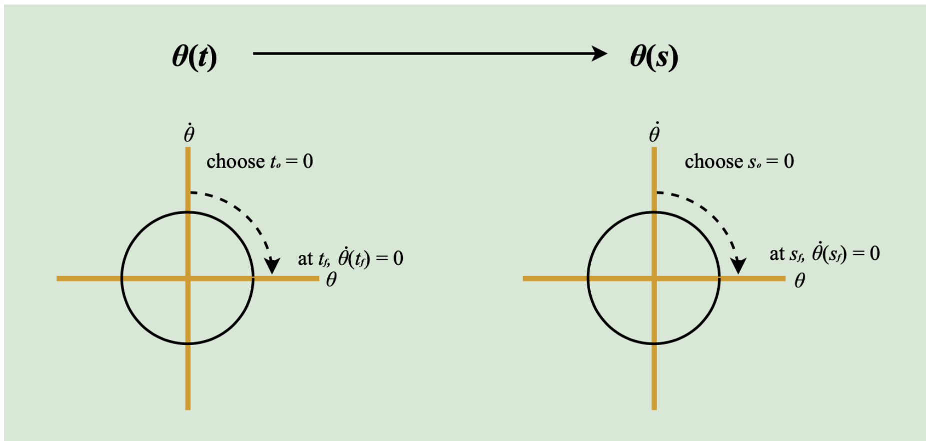

Figure 6: Our system of tiny hairs is analogous to the pendulum problem. We can consider $\theta(t)$ to be $\theta(s)$. In our system of the hair, acceptable energy values will be ones that correspond to a closed curve phase trajectory, similar to the oscillating pendulum.

Using conservation and initial conditions we can write

$$\mathcal{E}_0 = \frac{1}{2}\left(\frac{d\theta}{ds}\right)^2\Big|_{s=0} = \frac{1}{2}\left(\frac{d\theta}{ds}\right)^2 + \omega_\epsilon^2 \sin\theta \tag{28}$$

Note that we would be on the same energy surface if we started with initial velocity equal to zero at a value θ_0

$$\mathcal{E}_0 = \frac{1}{2}\left(\frac{d\theta}{ds}\right)^2\Big|_{s=0} = \omega_\epsilon^2 \sin\theta_0 \tag{29}$$

In the pendulum problem the potential is $-\cos\theta$ and the pendulum oscillates about $\theta = 0$. However, the boundary value problem for the hair is slightly different. We see that the pendulum's potential $-\cos\theta$ is shifted by $\pi/2$ from the hair's potential, $\sin\theta$. We can define the hair problem as analogous to a pendulum staring at $\theta = 0$, a distance up the potential well, and then project the pendulum further up the well with an initial velocity enough to hit its turning point at $d\theta/ds = 0$. We want to determine the initial value of $d\theta/ds$ corresponding to a time (length) for this to occur. To transform our problem to the pendulum problem we will shift θ by $\pi/2$.

$$\hat{\theta} = \theta + \tfrac{\pi}{2} \quad \Rightarrow \quad \sin(\theta) = -\cos(\hat{\theta})$$

$$\mathcal{E} = \frac{1}{2}\left(\frac{d\hat{\theta}}{ds}\right)^2 - \omega_\epsilon^2 \cos(\hat{\theta}) \tag{30}$$

By the double angle formula $\cos\theta = 1 - 2\sin^2(\theta/2)$. We can drop the the constant since it will not affect the potential.

$$\mathcal{E} = \frac{1}{2}\left(\frac{d\hat{\theta}}{ds}\right)^2 - \omega_\epsilon^2 \sin^2(\hat{\theta}/2) \tag{31}$$

Solving for $d\hat{\theta}/ds$ gives

$$\frac{d\hat{\theta}}{ds} = \sqrt{2\mathcal{E}}\sqrt{1 - \frac{2\omega_\epsilon^2}{\mathcal{E}}\sin^2(\hat{\theta}/2)} \tag{32}$$

Next we separate variables and integrate, with the integral with respect to $\hat{\theta}$ going from $\hat{\theta}(0) = \pi/2$ to $\hat{\theta}(s) = \theta(s) + \pi/2$

$$\sqrt{2\mathcal{E}}\int_0^s ds = \int_{\pi/2}^{\theta(s)+\pi/2} \frac{d\hat{\theta}}{\sqrt{1 - \frac{2\omega_\epsilon^2}{\mathcal{E}}\sin^2(\hat{\theta}/2)}} \tag{33}$$

$$\sqrt{2\mathcal{E}}s = \int_{\pi/2}^{\theta(s)+\pi/2} \frac{d\hat{\theta}}{\sqrt{1 - \frac{2\omega_\epsilon^2}{\mathcal{E}}\sin^2(\hat{\theta}/2)}} \tag{34}$$

we can define

$$k^2 = \frac{2\omega_\epsilon^2}{\mathcal{E}} < 1$$

and perform another change of variables

$$\tilde{\theta} = \tfrac{\hat{\theta}}{2} \quad \Rightarrow \quad 2d\tilde{\theta} = d\hat{\theta}$$

so that

$$\sqrt{\frac{\mathcal{E}}{2}}s = \int_{\pi/4}^{\theta(s)/2+\pi/4} \frac{d\tilde{\theta}}{\sqrt{1-k^2\sin^2(\tilde{\theta})}} \tag{35}$$

By breaking this integral we have

$$\sqrt{\frac{\mathcal{E}}{2}}s = \int_{0}^{\theta(s)/2+\pi/4} \frac{d\tilde{\theta}}{\sqrt{1-k^2\sin^2(\tilde{\theta})}} - \int_{0}^{\pi/4} \frac{d\tilde{\theta}}{\sqrt{1-k^2\sin^2(\tilde{\theta})}} \tag{36}$$

The second integral is an incomplete elliptic integral of the first kind, $F(\frac{\pi}{4}|k^2)$, for which we can find the value of.

$$\sqrt{\frac{\mathcal{E}}{2}}s + F\left(\frac{\pi}{4}|k^2\right) = \int_{0}^{\theta(s)/2+\pi/4} \frac{d\tilde{\theta}}{\sqrt{1-k^2\sin^2(\tilde{\theta})}} \tag{37}$$

We want to determine the solution to this of the form

$$\theta = \theta(\theta_0', \omega_\epsilon, s) \tag{38}$$

3.2 Determining the Solution Analytically

Consider Equation (37) at a specific energy value $\mathcal{E}_0$.

$$\sqrt{\frac{\mathcal{E}_0}{2}}s + F\left(\frac{\pi}{4}|k_0^2\right) = \int_{0}^{\theta(s)/2+\pi/4} \frac{d\tilde{\theta}}{\sqrt{1-k_0^2\sin^2(\tilde{\theta})}} \tag{39}$$

We know

$$\mathcal{E}_0 = \frac{1}{2}\left(\frac{d\theta}{ds}\right)^2 + \omega_\epsilon^2 \sin\theta \tag{40}$$

is true for any value of s due to conservation. Now considering the initial conditions

$$\theta(0) = 0 \quad \text{and} \quad \tfrac{d\theta}{ds}|_{s=0} =: \theta_0'$$

At $s = 0$

$$\mathcal{E}_0 = \frac{\theta_0'^2}{2} \tag{41}$$

while at $s = 1$, let $\theta(1) =: \theta_1$

$$\mathcal{E}_0 = \omega_\epsilon^2 \sin\theta_1 \tag{42}$$

Thus

$$\mathcal{E}_0 = \frac{\theta_0'^2}{2} = \omega_\epsilon^2 \sin\theta_1 \tag{43}$$

Evaluating Equation (39) at $s = 1$ gives

$$\sqrt{\frac{\mathcal{E}_0}{2}} + F\left(\frac{\pi}{4}|k_0^2\right) = \int_0^{\theta_1/2+\pi/4} \frac{d\tilde{\theta}}{\sqrt{1 - k_0^2 \sin^2(\tilde{\theta})}} \tag{44}$$

This will help us find how θ_0' is related to our boundary condition $\theta_1' = 0$ to get a formula for $\theta_0'(\omega_\epsilon)$. Equations 43 and 44 give us two equations with two unknowns: θ_1 and θ_0', involving a single parameter ω_ϵ, since $k_0^2 = 2\omega_\epsilon^2/\mathcal{E}_0$. Solving Equation (43) for θ_1 gives

$$\theta_1 = \sin^{-1}\left(\frac{\theta_0'^2}{2\omega_\epsilon^2}\right) \tag{45}$$

Plugging this into Equation (44) gives

$$\sqrt{\frac{\mathcal{E}_0}{2}} + F\left(\frac{\pi}{4}|k_0^2\right) = \int_0^{\frac{1}{2}\sin^{-1}\left(\frac{\theta_0'^2}{2\omega_\epsilon^2}\right)+\pi/4} \frac{d\tilde{\theta}}{\sqrt{1 - k_0^2 \sin^2(\tilde{\theta})}} \tag{46}$$

Jacobi Elliptic Functions are a set of functions that result from the inverse of elliptic functions [11]. Two of the Jacobi Elliptic Functions are the sn and

cn functions. If

$$u = F(\phi|k^2) = \int_0^{\phi} \frac{1}{\sqrt{1-k^2\sin^2\phi}} d\theta \tag{47}$$

then $sn(u,k) = \sin\phi$ and $cn(u,k) = \cos\phi$.

Operation on both sides with sn or cn gives

$$sn\left(\sqrt{\frac{\mathcal{E}_0}{2}} + F\left(\frac{\pi}{4}|k_0^2\right), k_0\right) = \sin\left(\frac{1}{2}\sin^{-1}\left(\frac{\theta_0'^2}{2\omega_\epsilon^2}\right) + \frac{\pi}{4}\right) \tag{48}$$

or

$$cn\left(\sqrt{\frac{\mathcal{E}_0}{2}} + F\left(\frac{\pi}{4}|k_0^2\right), k_0\right) = \cos\left(\frac{1}{2}\sin^{-1}\left(\frac{\theta_0'^2}{2\omega_\epsilon^2}\right) + \frac{\pi}{4}\right) \tag{49}$$

We will continue using sn. Since $k_0^2 = 2\omega_\epsilon^2/\mathcal{E}_0$, and $\mathcal{E}_0 = \frac{\theta_0'^2}{2} = \omega_\epsilon^2 \sin\theta_1$, the argument of the left hand side can be written in terms of θ_0' and ω_ϵ.

$$sn\left(\frac{\theta_0'}{2} + F\left(\frac{\pi}{4}|\frac{4\omega_\epsilon^2}{\theta_2'^2}\right), k_0\right) = \sin\left(\frac{1}{2}\sin^{-1}\left(\frac{\theta_0'^2}{2\omega_\epsilon^2}\right) + \frac{\pi}{4}\right) \tag{50}$$

Now we have an expression that relates θ_0' and ω_ϵ. We can solve for $\theta_0'(\omega_\epsilon)$ using numerical methods, such as Newton's Method. Then our solution (Equation (38)) can be written as a function that varies with ω_ϵ and s.

$$\theta = \theta(\theta_0'(\omega_\epsilon), \omega_\epsilon, s) = \theta(\omega_\epsilon, s) \tag{51}$$

Plugging this back into our relation for $\omega^2/\omega_\epsilon^2$ from Equation (24) we can find

$$\frac{\omega^2}{\omega_\epsilon^2} = 1 - \epsilon \int_0^1 \cos\left(\theta(\theta_0'(\omega_\epsilon), \omega_\epsilon, s')\right) ds' = \Upsilon(\omega_\epsilon, \epsilon) \tag{52}$$

Recall that $\epsilon = \frac{H}{L}$ is determined by the apparatus of the experiment. If we can find a solution for ω_ϵ from this numerically, then we will have the solution that only depends on s.

$$\theta = \theta(s) \tag{53}$$

This solution describes the shape of the hair subject to shear-driven Stokes flows in terms of the angle it differs from vertical at every point along the hair s.

We have reduced the problem to a numerical problem by way of the analytical method explained above.

References

[1] Alvarado, J., Comtet, J., de Langre, E. et al. *Nonlinear flow response of soft hair beds.* Nature Phys 13, 1014{1019 (2017). https://doi.org/10.1038/nphys4225

[2] Vogel, S. Davis, K. K. textitCats' Paws and Catapults: Mechanical Worlds of Nature and People

[3] Uruba, Vaclav. (2018). *On Reynolds number physical interpretation.* AIP Conference Proceedings. 2000. 020019. 10.1063/1.5049926.

[4] Audoly, B. Pomeau, Yves. (2008). textit Elasticty and geometry: from hair curls to the nonlinear response of shells.

[5] Roussel, Marc R. *Hamiltonian Systems.* uleth.ca, University of Lethbridge, 25 Oct. 2005, people.uleth.ca/ roussel/nld/Hamiltonian.pdf.

[6] Culham, J. R. *Elliptic Integrals, Elliptic Functions and Theta Functions.* Mhtlab.uwaterloo, www.mhtlab.uwaterloo.ca/courses/me755/web$_chap3.pdf$.

[7] Beléndez, Augusto Villalobos, Carolina Méndez, David Vázquez, Tarsicio Neipp, Cristian. (2007). *Exact solution for the nonlinear pendulum.* Revista Brasileira de Ensino de Física. 29. 10.1590/S0102-47442007000400024.

[8] M. Abramowitz and I. A. Stegun, In: M. Abramowitz and I. A. Stegun, Eds., Dover *Handbook of Mathematical Functions: With Formulas, Graphs, and Mathematical Tables* In: M. Abramowitz and I. A. Stegun, Eds., Dover Books on Advanced Mathematics, Dover Publications, New York, 1965. Butikov, Eugene. (1999).

[9] Rubinsztejn, Ari. *An Introduction to Phase Portraits.* Gereshes, 6 Mar. 2019, gereshes.com/2019/03/04/an-introduction-to-phase-portraits/.

[10] Butikov, Eugene. (1999). *The rigid pendulum - an antique but evergreen physical model.* European Journal of Physics. 20.

[11] *Jacobi Elliptic Functions.* From Wolfram MathWorld, mathworld.wolfram.com/JacobiElliptic Functions.html.